

# Al motion rates in levitated, molten Al<sub>2</sub>O<sub>3</sub> samples, measured by pulsed gradient spin echo <sup>27</sup>Al NMR

R.F. Marzke<sup>a,\*</sup>, J. Piwowarczyk<sup>a</sup>, P.F. McMillan<sup>b</sup>, G.H. Wolf<sup>c</sup>

<sup>a</sup> Department of Physics and Astronomy, Arizona State University, Tempe, AZ 85287-1504, USA

<sup>b</sup> Royal Institution of Great Britain, Davy-Faraday Research Laboratory, 21 Albemarle St., London W1S 4BS, UK

<sup>c</sup> Department of Chemistry and Biochemistry, Arizona State University, Tempe, AZ 85287-1504, USA

## Abstract

Strong attenuation of <sup>27</sup>Al NMR signals has been observed in a magnetic field gradient, in beads of alumina melted by a CO<sub>2</sub> laser and levitated in flowing Ar. The standard NMR diffusivity measurement interpretation of the data leads to very large ( $\sim 1.5 \times 10^{-7}$  m<sup>2</sup>/s) effective diffusivity values, approximately independent of temperature between melting and 2500 °C. These high values and their weak temperature dependence contrast sharply with estimates of ionic diffusivity arising from the known, activated temperature dependences of molten alumina's viscosity and <sup>27</sup>Al NMR line width. Our anomalously large diffusivities are attributed to bulk displacive motions, which can be visually observed in the levitated molten beads and can lead to substantial Al displacements over experimental NMR time scales. Possible origins of these motions are briefly discussed.

© 2005 Elsevier Ltd. All rights reserved.

**Keywords:** Diffusion; Spectroscopy; Al<sub>2</sub>O<sub>3</sub>; Refractories; NMR

## 1. Introduction and background

Rapid advances in applications for refractory oxides have led to the development of new approaches in the study of these materials' chemical and physical properties. Among the methods introduced since the late 1980s is NMR of the abundant <sup>27</sup>Al nucleus, in molten, aluminum-containing ceramics. Measurements of <sup>27</sup>Al NMR chemical shift dependences upon sample composition have been extensively carried out on a number of molten ceramics.<sup>1–6</sup> The value of the chemical shift depends largely upon the nearest neighbor environment of the active nuclei, and thus its measurement provides a direct probe of the local chemical bonding.

In this paper we have attempted to extend the application of NMR beyond chemical shift measurements to include direct measurements of Al mobilities in gas flow-levitated molten ceramic beads. We have employed a well-established NMR technique, based upon application of a pulsed magnetic field

gradient to a sample placed in the large DC magnetic field of a superconducting NMR magnet, first introduced by Stejskal and Tanner.<sup>7</sup> This technique is normally used over modest ranges of temperature in the measurement of the intrinsic diffusivities of individual atoms, ions or molecules, for liquid samples in stationary containers. In the containerless melting approach required for NMR in refractory systems, the samples are not stationary and are subject to additional coherent and incoherent motions. Examples of such motions are bulk sample oscillations and rotations, as well as bulk macroscopic mass flows, e.g. convection. These factors may contribute to the inferred or "effective" diffusivities derived from our experiments. We report herein our initial results for rates of incoherent Al motions measured in argon gas-levitated bulk samples of the important ceramic alumina, Al<sub>2</sub>O<sub>3</sub>.

The NMR of <sup>27</sup>Al in molten ceramics was first observed by a group at the University of Orleans.<sup>1–4</sup> Their findings were mainly based upon sensitive determinations of the <sup>27</sup>Al chemical shift, measured with respect to the standard NMR frequency of <sup>27</sup>Al for the aqueous Al<sup>3+</sup> ion. Measurement of the chemical shift of a given nucleus in any liquid is made

\* Corresponding author.

E-mail address: [Robert.Marzke@asu.edu](mailto:Robert.Marzke@asu.edu) (R.F. Marzke).

possible by the rapidity with which an individual atom moves. The very fast hopping motion of the atom in the liquid relative to the NMR timescale (in the range 75–100 MHz) effectively gives a time-averaged picture of the local environment for the atom. This time-averaging narrows the broad  $^{27}\text{Al}$  NMR line typical of a solid, down to a width of approximately 100 Hz or less. The motional narrowing yields a relatively well-defined value of the chemical shift for ceramic liquids, much as for other NMR lines in many liquid compounds at ordinary temperatures.

Decades prior to this development, however, NMR's application to the study of diffusion had been initiated by Hahn,<sup>8</sup> then further developed by Carr and Purcell<sup>9</sup> and by Torrey.<sup>10</sup> In their approach, a steady magnetic field gradient is imposed upon a liquid sample held in a fixed container. The resulting additional attenuation of the NMR signal can be directly related to the self-diffusion constant of a given atom or molecule. Hahn et al. first exploited this effect to measure diffusivities in water and other molecular liquids, over normal laboratory temperature ranges. Later, Stejskal and Tanner developed a much more powerful technique employing a pulsed magnetic field gradient, which is widely used today. It is this approach that we have attempted to apply in the ultra-high temperature containerless experiments. Among the salient features of NMR-based diffusion measurements are their capabilities for yielding diffusivity values quickly over a broad temperature range, and for monitoring diffusion of different atomic constituents of many kinds of samples (e.g. molecular liquids or electrolytes). The method requires no rare or expensive isotopes, and is one of the few available for directly determining the diffusivity of Al in melts of aluminum-containing ceramics.

The physical basis for NMR's sensitivity to diffusion can be understood from the well-known linear dependence of a nuclear spin's precession frequency upon the strength of the local magnetic field, at the spin's exact position in the laboratory reference frame. In the presence of a field gradient this frequency will vary when the position of the spin changes, as happens when the spin belongs to a chemical species undergoing diffusive or bulk motions in a liquid. In a sample containing  $\sim 10^{22}$  such moving spins, random atomic motions result in a spreading of the individual precession motions displayed by each atom. This causes the ensemble coherence of spin orientations to be rapidly destroyed, leading to an NMR signal decaying according to an exponential law with time to the third power, i.e. as  $\exp(-\alpha t^3)$ . The decay constant  $\alpha$  depends upon the magnitude of the magnetic field gradient, the nucleus under observation and the diffusivity of the chemical species. In the presence of large field gradients this effect can dominate all other sources of observed NMR signal intensity decay.

Prominent among these other sources is the  $T_1$  nuclear spin relaxation, which over measurable experimental time scales returns an ensemble of precessing spins back to its thermal equilibrium alignment along the DC magnetic field, but with a linear exponential time dependence. Also, as noted above

for molten ceramics the very high temperatures involved lead to sufficiently fast ionic diffusion to produce a relatively narrow NMR line for  $^{27}\text{Al}$ . This means that the exponential  $T_2$  decay of the nuclear magnetization in the plane of precession, approximately equal to  $T_1$  in liquids, is quite fast, since both decays primarily arise from the Al nucleus' electric quadrupole moment interaction with rapidly fluctuating local electric field gradients. Relatively large external magnetic field gradients are thus required for molten Al-containing ceramics, in order to produce measurable motion-caused signal attenuations following the  $\exp(-\alpha t^3)$  law, within the experimental time scale fixed by the nuclear relaxation ( $\sim 3T_2$ ) at high temperatures.

## 2. Experimental

Detailed accounts of the pulsed gradient spin echo NMR diffusometry technique may be found in the standard NMR literature, but here we will briefly sketch its primary principles and outline its adaptation for ultra high-temperature operation in our experiment. To review, in modern instruments NMR spectra are usually obtained by applying a single short, high-power radio frequency pulse  $H_1$  to a sample in a spectrometer, along an axis perpendicular to the large DC magnetic field  $H_0$ . The effect of this pulse, and of all other radio frequency pulses, can be shown to be the same as a rotation of the sample's assembly of nuclear magnetic moments, i.e. its nuclear magnetization. The axis of this rotation, however, also rotates in the plane perpendicular to the DC field, at the frequency of the r.f. pulse. Its effect on the nuclear magnetization is therefore most easily visualized by viewing the experiment in a frame of reference rotating at this frequency, known as the "rotating frame".

In the rotating frame the radio frequency magnetic field  $H_1$  is at rest and the magnetization "sees" a stationary effective magnetic field. When the r.f. pulse's frequency is at or very close to the Larmor frequency,  $\omega_L = \gamma H_0$ , of the nuclear spin, this effective field consists mainly of the r.f. field  $H_1$ , which is oriented perpendicular to the DC field. In the rotating frame the  $H_1$  field then rotates the bulk magnetization away from the DC field's direction, by an angle that increases linearly with time and also depends linearly upon the strength of  $H_1$ . After a typical period of a few microseconds, the bulk magnetization has rotated by  $90^\circ$  and precesses in the laboratory frame at approximately the Larmor frequency in a plane perpendicular to the DC field. At this point the r.f. pulse may be turned off, and the rotating macroscopic magnetization induces a signal in a radio frequency coil (usually the same coil used to apply the r.f. pulse) via Faraday's law of electromagnetic induction. The signal eventually decays to zero as the individual nuclear spins "dephase" and ultimately relax back to thermal equilibrium. Fourier transformation of this decaying time-domain signal then directly yields the standard NMR spectrum of the sample, which has at least as many different NMR frequencies present as there

are chemically inequivalent nuclei in the sample under observation.

The r.f. pulse need not be cut off at a  $90^\circ$  rotation, however, but may instead be continued for as long as desired. For example, if the pulse lasts for twice the  $90^\circ$  duration, it produces a  $180^\circ$  spin rotation, inverting the initial magnetization. This capability for rotating spin magnetizations by any amount was used to great advantage by E.L. Hahn, who introduced a sequence consisting of an initial  $90^\circ$  pulse first, followed after a variable time interval  $\tau$  by a  $180^\circ$  pulse. It can be understood that the effect of the  $180^\circ$  pulse is essentially to reverse the dephasing effect that acts upon the nuclear spin ensemble following the  $90^\circ$  pulse. As a result of the  $180^\circ$  pulse, signals from different parts of the ensemble's magnetization will then recombine constructively, producing an induced radio frequency signal with a peak value at a time  $2\tau$ . The  $180^\circ$  pulse is called a refocusing pulse, and the signal is called a spin "echo". The echo may be recorded and Fourier transformed, yielding an NMR frequency spectrum. A diagram showing this fundamental experiment is given in Fig. 1a.

Obtaining spectra from spin echoes has both advantages and limitations, as discussed in the literature. It is particularly useful, however, in making diffusion measurements. To employ this pulse sequence for measurement of diffusion in a magnetic field gradient, Stejskal and Tanner incorporated two successive gradient pulses of variable length  $\delta$  and of exactly equal strengths, each pulse following one of the two r.f. pulses ( $90^\circ$ , then  $180^\circ$ ), as diagrammed in Fig. 1a and b. The effect of the gradient is to cause each spin, as it hops diffusively, to experience a random change in its precession frequency. This random fluctuation contributes to the dephasing and consequent attenuation of the NMR signal. The second gradient pulse acts in concert with the  $180^\circ$  radio frequency (r.f.) refocusing pulse to undo any coherent dephasing effect of the first gradient pulse. Either the length or the magnitude of the gradient pulse pair can be varied, as can the interpulse delay time,  $\tau$ . The resulting signal attenuation of the spin echo signal can be analyzed, in a manner discussed below, yielding a value

for the rate of incoherent, random motions, such as diffusion, that occur in a sample. The great advantage of using pulsed field gradients is that they may be applied for durations long enough to produce measurable motional attenuation, but are then turned off during signal acquisition, allowing the attenuated NMR spin echo signal of the nuclei under observation to be fully recorded and Fourier transformed.

For our experiment, we designed a special NMR probe in which a spherical sample of approximately 3 mm diameter is levitated in a flow of Ar gas, inside the 89 mm bore of the superconducting magnet of an NMR spectrometer. A  $\text{CO}_2$  laser is directed down the bore, producing sample temperatures well above  $2000^\circ\text{C}$ .<sup>1–3</sup> The diameter of the sample is chosen to be optimal for: (1) the diameter of the magnet bore, (2) good NMR signal-to-noise ratio, (3) the laser power available, and (4) ease and stability of containerless levitation of the molten sample.

To enable incoherent motion measurements a separate set of coils, in addition to those generating radio frequency magnetic fields, must be furnished to produce pulsed magnetic field gradients at the sample. These are similar to Helmholtz coils, but carry current in opposing senses, which leads to a highly uniform magnetic field gradient. They are known as anti-Helmholtz coils, and they must be shielded against interaction with the superconducting magnet's currents by a second set of coils, wound on a larger diameter.<sup>11</sup> The resulting gradient values are controlled by the first and second coil sets' geometry and by the value of current. The use of large ( $\sim 15$  A) millisecond-length current pulses allows application at ultra-high temperatures of the above-outlined pulsed gradient spin echo (PGSE) NMR approach to the measurement of rates of Al incoherent motions.

### 2.1. Levitator and laser heating

For sample levitation, a 10 mm o.d. nozzle was machined from a single length of BN rod, with an internal convergent–divergent constriction. Very low ( $<1$  l/min) Ar gas flows are controlled electronically, at rates adjusted for optimal stability of the molten sample, which is viewed through a digital camera. With the sample levitating in position just above the nozzle constriction, the flowing gas passes through a narrow annular opening at the closest approach of the sample to the nozzle. Estimated flow velocities here may reach substantial values, of order 10 m/s, as required to support the weight of the sample under flow conditions. Sample heating is provided by a Synrad Evolution 125 laser, with 125 W nominal maximum power output. To date we have not focused the beam, which has a nominal 4 mm waist. The beam is square-wave modulated, the fraction of a cycle with beam on being continuously variable, for fine control of average power output. The laser is operated in this mode for all measurements, and is not switched off during data acquisition as in time-resolved experiments.<sup>12</sup> Conservative design of the high-temperature section of the NMR probe, using multiple cooling air streams for interior parts made

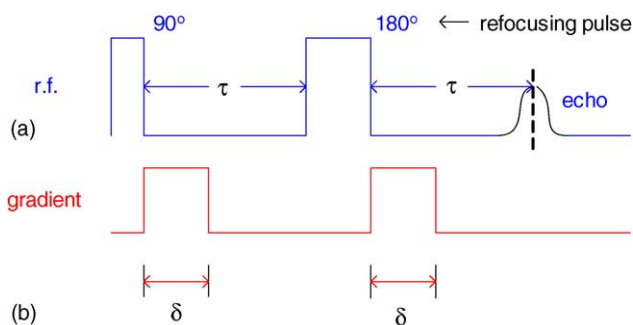


Fig. 1. (a) The two-pulse spin echo sequence. (b) The gradient pulses, shown as they are applied during the spin echo sequence.<sup>7</sup> The strength of each gradient pulse is controlled by the magnitude of the gradient pulse current and by the geometry of the coils through which this current passes, in the NMR probe. The length  $\delta$  of each pulse is variable.

from Vespel, allows stable, uninterrupted signal acquisition for periods up to several hours in length.

## 2.2. Temperature

Temperatures are measured using the technique of spectroradiometry, in which an optical spectrum of the light emitted by a sample is acquired and fitted to a grey-body spectrum over a broad range of wavelengths.<sup>13,14</sup> A wavelength-averaged emissivity is factored in directly, where values for this quantity are known for the spectral range covered. In our experiment, light emitted from the sample is transmitted via a light pipe to an Acton 300 mm focal length optical spectrometer, equipped with a thermoelectrically cooled Princeton Instruments CCD detector. The spectrum is fitted over the wavelength range 250–750 nm to a Planck expression multiplied by an average emissivity, the only adjustable parameters being a constant additive background and the temperature in the Planck law itself. Calibration is made against a tungsten radiance standard, whose UV–vis spectrum corresponds to an effective temperature of 2850 °C. Using the full output of the 125 W laser, the highest temperatures attainable for our 3 mm diameter ceramic samples are of order 2500 °C.

Temperature calibration is regularly checked against observation of the melting of alumina, in two ways. One is by direct viewing of the sample via the above-mentioned digital camera. When fully molten, the sample appears as a stable, uniform sphere, while in the partially molten or solid state random motions are easily visible, arising from frequent contacts with the levitator nozzle's upper (diverging) surface. A second, more precise indicator of melting is the appearance of the motionally narrowed (~130–200 Hz width) NMR line for <sup>27</sup>Al, which can occur only if the sample is at least partially liquid. Alumina melts are known to be capable of undercooling by as much as several hundred degrees upon solidification, so observations of melting are taken during heating of samples. Liquid alumina is also known to have high values of emissivity near melting, at wavelengths commonly used in optical pyrometry.<sup>15</sup> In our experience, the melting point of alumina determined using either of these approaches is, within error ( $\pm 25$  °C), consistent with an emissivity close to 1.0.

Sample temperature measurements in levitation experiments raise questions concerning temperature gradients, which some studies indicate can be as large as several hundred degree centigrades.<sup>16,17</sup> NMR tests have been conducted, but so far temperature gradients of this magnitude have not been observed. In one of these tests the possibility of partial liquefaction was investigated, via a search for solid material in the cooler regions of a sample. At a temperature well above melting 16,000 sweeps were averaged, with the spectrometer adjusted for optimal, background-free signal detection of <sup>27</sup>Al in solid Al<sub>2</sub>O<sub>3</sub>. No broad component of the intense Al line was observed. Taken together, all evidence to date indicates that the spectroradiometric approach yields molten sample

temperatures reliably, in the case of alumina to within measurement error ( $\pm 25$  °C) of its melting temperature (2050 °C).

## 2.3. NMR line widths and relaxation times

A Varian Chemagnetics 300 MHz wide-bore solids NMR instrument was used, with a highly uniform magnetic field shimmed to a residual <sup>27</sup>Al line width of ~8 Hz. This width is small compared to the typical 100–200 Hz widths commonly observed for molten ceramics in the high temperature probe (constructed using aluminum-free tuning elements to yield negligible <sup>27</sup>Al background signals). The frequency of an observed <sup>27</sup>Al line, i.e. its chemical shift, was thus readily determined, in the absence of an applied magnetic field gradient. A ~1 M Al(NO<sub>3</sub>)<sub>3</sub> solution was used as an NMR frequency reference for the shifts, following standard Al solution NMR practice. In addition, the short (~5 ms), quadrupolar <sup>27</sup>Al spin relaxation times  $T_1$  and  $T_2$  were directly measured using standard 2-pulse sequences, and were found to be essentially independent of temperature. From observed  $T_2$  values the spin lifetime contribution to the <sup>27</sup>Al line width was found to be ~35 Hz. Other line width contributions have also been estimated, from the widths of <sup>7</sup>Li lines observed in the ultra high-temperature probe, after tuning to the resonant frequency for this nucleus during calibration of the probe's magnetic field gradient (see below). These widths, of the very narrow line of <sup>7</sup>Li in LiCl solutions, indicate that most of the observed breadth of NMR lines in the probe arises from magnetic field inhomogeneity, despite the sample's spherical shape. This may be expected from the non-uniform geometry of the levitator's BN nozzle, in the immediate vicinity of the sample. During the work reported here, line widths were monitored but varied only slightly, and were found to play no role in incoherent motion measurements.

## 2.4. Gradient calibration

The central requirement for NMR determinations of incoherent motional rates is knowledge of the magnetic field gradient in the probe. In our data acquisition the duration of the simple, rectangular gradient current pulses is varied while its amplitude remains constant, necessitating only a single gradient determination for calibration. For this purpose we employed a second probe, regularly used in pulsed gradient spin echo measurements of diffusivities in liquid electrolytes over standard temperature ranges<sup>18,19</sup> and calibrated against the known diffusivity of highly pure water.<sup>20</sup> Samples were placed in supported, uniform 5 mm diameter tubes, and residual <sup>7</sup>Li line widths were as low as 2 Hz for this probe. With it we determined the ionic diffusivity at room temperature of Li<sup>+</sup> in a 2 M solution of LiCl. Then, placing a sample of the solution in the ultra high temperature probe (tuned to <sup>7</sup>Li), we measured a gradient strength of  $0.277 \pm 0.015$  T/m at the selected pulsed current value, approximately 15 A. During this measurement the

LiCl solution remained at room temperature, but the gradient coil and probe cooling airflow settings in the probe were identical to those later used for  $^{27}\text{Al}$  incoherent motion measurements at high temperatures. For those measurement runs, described below, the gradient current amplitude was monitored for changes as laser heating power was applied. No variation has been observed. Finally, a calculation of the gradient made directly from the Biot–Savart law yielded values well within error of our experimental finding.

### 2.5. Procedure

As stated above, data are obtained in the pulsed gradient spin echo experiment by varying the gradient pulse's length  $\delta$  while the  $^{27}\text{Al}$  signal intensity  $I(\delta)$  is recorded over more than a decade. The spin echo r.f. pulse pair separation  $\tau$  is held constant, at a value that is selected to maximize diffusive signal attenuation, longer  $\tau$  values resulting in stronger attenuation. The data are fitted to the following equation for the amplitude of the spin echo signal from a diffusing species, originally derived by Stejskal and Tanner:<sup>7</sup>

$$I(\delta) = I_0 \exp\left(-\gamma^2 D g^2 \delta^2 \left(\frac{\tau - \delta}{3}\right)\right)$$

Here,  $I_0$  is the signal intensity with zero applied gradient pulse,  $D$  is the diffusivity of the chemical species containing the nucleus under observation, i.e. that of the Al ion in the melt, while  $g$  is magnetic field gradient (in Tesla/m).  $\gamma$  is the gyromagnetic ratio of the  $^{27}\text{Al}$  nucleus, which is the ratio between the applied magnetic field  $H$  and the  $^{27}\text{Al}$  Larmor precession frequency  $\omega$ , as given in the basic Larmor equation of NMR:

$$\omega_L = \gamma H$$

The range of usable  $\tau$  values for this measurement in our samples of alumina is limited, owing to the rapid (4–5 ms) spin-spin ( $T_2$ ) and spin-lattice ( $T_1$ ) relaxation times for  $^{27}\text{Al}$  in a molten ceramic, as mentioned in the introduction. These short times also mandate use of the largest practical gradient currents, which are furnished by a HEXFET-controlled pulsed power supply of our own design. Signals are normally averaged for 64 sweeps at short  $\delta$  ( $\sim 1$  ms) values, where the attenuation is small, the number of sweeps increasing to 512 as  $\delta$  is lengthened.

A typical logarithmic plot of  $^{27}\text{Al}$  signal intensity  $I$  versus the quantity  $\delta^2(\tau - \delta/3)$  is shown in Fig. 2. From the above equation it is seen that a straight line should be obtained. The slope of the fitted line is the product of three factors: the square of the gyromagnetic ratio  $\gamma$  of the  $^{27}\text{Al}$  nucleus, the diffusivity  $D$  and the square of the magnetic field gradient  $g$ . With the field gradient known, a value for  $D$  is readily obtained by fitting the signal intensity data at each sample temperature. In measurements over normal temperature ranges on stationary liquid samples  $D$  is the individual ionic or molecular diffusivity, no other source of random motions for the Al nuclei being available. With levitated samples, however, the derived  $D$  is

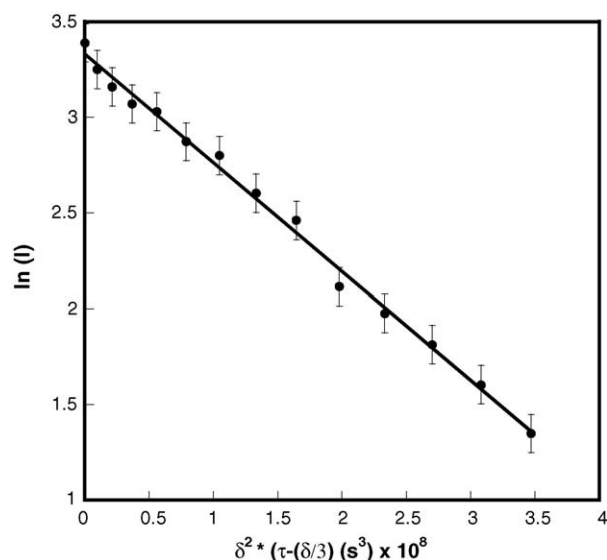


Fig. 2. Stejskal–Tanner plot of the natural logarithm of  $^{27}\text{Al}$  signal intensity in alumina, at 2088 °C.

actually an effective diffusivity, and account must be taken of quasi-bulk motions such as convective flows and random sample rotations. These can be a source of random motions for the Al nucleus, as discussed below.

### 3. Results

Measurements of the effective diffusivity of Al in levitated, molten alumina beads, calculated from spin echo decay plots like that of Fig. 2, have been performed over the temperature range 2050–2450 °C. These show an approximately constant  $D_{\text{eff}}$  value of  $1.5 \times 10^{-7}$  m/s<sup>2</sup> (to within 20%), as seen in Fig. 3. For comparison, this value is almost two orders of magnitude greater than the diffusivity of water at room

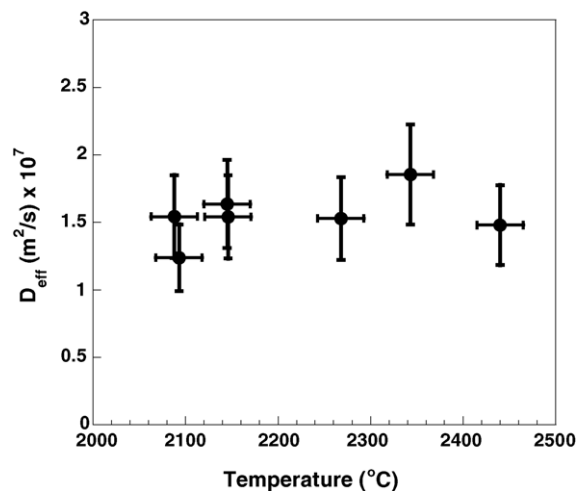


Fig. 3. Effective diffusivity of Al in molten, levitated alumina beads vs. temperature, from Stejskal–Tanner plots for temperatures ranging from melting to 2450 °C.

temperature.<sup>20</sup> Although the number of data points taken to date is not large, no significant variation in effective diffusivity has been observed over the temperature range. The random motions responsible for the spin echo decays thus do not appear to change between melting and 2450 °C.

Also measured in this study were values of the <sup>27</sup>Al chemical shift in alumina and spin relaxation times  $T_1$  and  $T_2$ . Like the effective diffusivity, these quantities remained constant over the temperature range within error, the shift being  $58.2 \pm 0.3$  ppm while the  $T_1$  and  $T_2$  values were respectively  $4.8 \pm 0.3$  and  $4.1 \pm 0.3$  ms.<sup>5,6</sup>

#### 4. Discussion

These results raise two principal questions: why is the NMR-measured effective diffusivity of Al in alumina samples so large for the levitated samples, and why is its temperature dependence so small? For comparison, values of the diffusivity may be estimated from the bulk viscosity,  $\eta$ , measured in the 1960s by Rossin et al.<sup>21</sup> in a container with the sample exposed to air, via the Stokes–Einstein relation:

$$D = \frac{kBT}{6\pi a\eta}$$

as discussed by Scamehorn and Angell.<sup>22</sup> Our effective diffusivity values measured via NMR are at least an order of magnitude larger than those inferred from the viscosity measurements. The Stokes–Einstein values also exhibit a temperature-dependent activated behavior, with an activation energy of 120 kJ/mol. In spin-relaxation time measurements based upon observed breadths of Al NMR lines, which were performed using time-resolved ultra high-temperature NMR with levitation in air, Florian et al. find similar activated behavior, with an activation energy of 130 kJ/mol.<sup>17</sup> At these activation energies our NMR-measured diffusivity at 2400 °C would be approximately twice that at 2100 °C, a trend that is clearly not reproduced.

Accepted models for the origins of observed viscosity dependences upon composition in silica–alumina and calcium–alumina melts are based mainly upon the extent of bonding of the diffusing oxygen with Al.<sup>23–26</sup> The role of extremely rapid motions of individual aluminum ions, like those measured by NMR, is rarely considered. Below we consider factors that may be responsible for our surprising findings.

1. As noted previously, there are other incoherent motions besides diffusion occurring in levitated samples, which can produce decays of the <sup>27</sup>Al spin echo amplitude in pulsed gradient NMR experiments. Among these are random rotations and/or convection currents, which have been directly observed by our group, by Weber et al.<sup>15,27</sup> and by Coutures et al.<sup>16</sup> In order to assess the effect of sample rotations, we performed an experiment in which the molten alumina sample was heated and then cooled quickly below melting, resulting in the sample's sticking

to the levitator's BN wall. Reheating does not release the sample, when such sticking occurs. (The sample must be completely cooled and removed by hand at room temperature.) Upon reheating, diffusion data like those of Fig. 2 were then taken, on the stuck sample. The results were basically identical to those of Fig. 2, showing that convective currents must be more important than rotations, as sources of Al motions in our samples.

An estimate can be made of the effective rotational  $D_r$  associated with these bulk currents, from observations of the motions of landmarks on the surface that become easily visible when the sample's temperature is close to melting. Assuming that these surface motions are representative of currents within the bulk, and considering the well-known Einstein relation:

$$\Delta s^2 \cong 6D_r \Delta t$$

we may identify  $\Delta s$  with an observed average displacement of a landmark over a time interval  $\Delta t$ . A typical displacement of  $\sim 0.5$  mm, occurring in a time interval  $\Delta t \sim 0.2$  s corresponds to a motional frequency of about 5 Hz<sup>16</sup> and yields a diffusivity estimate of order  $10^{-7}$  m<sup>2</sup>/s, in the neighborhood of our measured values. The effects of such motions, arising from convective currents, thus appear to be capable of dominating effects due to individual Al ion diffusion, even at the highest temperatures we can achieve. The reason for this dominance apparently lies in the relatively large size of observed displacements  $\Delta s$  near melting. Our NMR measurements then indicate that these motions change little in average amplitude or frequency, as sample temperature is increased.

The bulk motions may themselves arise from either or both of two sources. One is thermal gradients across the levitated sample, as discussed by Coutures et al.<sup>16</sup> Over the temperature range of our experiments these gradients should not be extreme, yet they may nevertheless engender convective currents, despite the small sample diameter. A second source has been suggested by Weber, who notes that velocities of the levitating Ar flow through the narrow ( $\sim 10$   $\mu$ m width) annular region between the sample and the levitator wall are quite high, of order 10 m/s. This flow velocity around the sphere of liquid alumina, whose viscosity is approximately that of water, may couple to the surface and excite waves, oscillations or even flows in the bulk of the drop.<sup>28</sup> In this situation the Ar flow itself would be considered a driving force for the production of bulk currents.

There exist means for assessing the role of convection effects in the NMR measurement of Al diffusivities in melts, by the use of bipolar, shaped magnetic field gradient pulses. This approach is well known in magnetic resonance imaging, where such shaped pulses can be employed to attenuate bulk motion artifacts.<sup>29–31</sup> They may also be employed to directly image velocities, in samples with flowing fluids. A present we are developing this capability for one-dimensional pulsed gradient diffusivity

measurement experiments. We will also examine the effects of varying the viscosity of the sample under study, and will extend these motional studies past alumina to other aluminum-bearing ceramics, for example members of the YAG and  $\text{Al}_2\text{O}_3$ –monazite families.

2. It should also be noted that a factor capable of strongly influencing ionic Al motions in a molten bead is the composition of the levitation gas, especially with regard to oxygen. This factor's effects are not well understood, but they have been reported by Weber et al.,<sup>15,27</sup> who measured spectral absorption coefficients and sample solidification behavior under weak reducing and oxidizing conditions. Even the morphology of samples levitated in Ar differed from that of samples studied in  $\text{O}_2$ , although Weber et al. did not observe such features as the macroscopic-sized cavities formed during Ar levitation reported by earlier workers.<sup>32</sup>

Strong effects of levitation gas composition have also been noted by Coutures et al.,<sup>16</sup> who studied high-temperature NMR of  $^{27}\text{Al}$  as well as thermal properties of alumina melts. These authors observed partial reduction of samples levitated in Ar at extremely high temperatures, leading to the presence of  $\text{Al}^0$  and bulk metallic aluminum in the interiors of quenched samples. Unlike Weber et al., this group found that large cavities persistently formed in samples levitated in Ar, presumably because of loss of oxygen and subsequent formation of metallic aluminum. In addition, they observed very large shifts in the positions and widths of  $^{27}\text{Al}$  NMR lines under strong heating in Ar.

We have not observed to date any line shifts or broadenings in Ar comparable to those reported by Coutures et al. Also, we see no evidence of cavities or voids in our samples. Our maximum temperature being limited to  $\sim 2500^\circ\text{C}$  by available laser power, we may have been unable to heat sufficiently to produce cavity formation or interior metallization in our samples.

## Acknowledgements

This work was co-funded by the National Science Foundation and the Air Force Office of Scientific Research, under NSF grant DRM01-116361. Additional support has been provided by AFOSR, under grant F4962-03-1-0346 and by the Research Corporation, under grant RA-0276. We wish to thank K. Schmidt for essential calculations in the design of the magnetic field gradient and shielding coils. We also thank R. Weber for many helpful discussions and suggestions.

## References

1. Massiot, D., Taulelle, F. and Coutures, J.-P., Structural diagnostic of high temperature liquid phases by  $^{27}\text{Al}$  NMR. *Colloq. Phys. C5*, 1990, **51**(Suppl. 18), 425.

2. Coutures, J.-P., Massiot, D., Bessada, C., Echegut, P., Rifflet, J.-C. and Taulelle, F., Etude par RMN  $^{27}\text{Al}$  d'aluminates liquides dans le domaine 1600–2100 °C. *C.R. Acad. Sci. Paris*, 1990, **310**, 1041.
3. Taulelle, F., Coutures, J.-P., Massiot, D. and Rifflet, J.-C., High and very high temperature NMR. *Bull. Magn. Reson.*, 1990, **11**, 314.
4. Poe, B. T., McMillan, P. F., Coté, B., Massiot, D. and Coutures, J.-P., Magnesium and calcium aluminate liquids: in situ high-temperature  $^{27}\text{Al}$  NMR spectroscopy. *Science*, 1993, **259**, 786–788.
5. Piwowarczyk, J., *Aluminum-27 Nuclear Magnetic Resonance Study of Molten Aluminum-bearing Oxides*, M.S. Thesis, Arizona State University, May 2001.
6. Marzke, R. F., Piwowarczyk, J., Boucher, S., Takulapalli, B., Wolf, G. H., McMillan, P. F. et al., Melt and glass structure in the  $\text{Al}_2\text{O}_3$ –CaO–LaPO<sub>4</sub> system studied by  $^{27}\text{Al}$  and  $^{31}\text{P}$  NMR, and by Raman scattering. *J. Eur. Ceram. Soc.*, 2005, **25**, 1333–1340.
7. Stejskal, E. O. and Tanner, J. E., Spin diffusion measurements: spin echoes in the presence of a time-dependent field gradient. *J. Chem. Phys.*, 1965, **42**, 288–292.
8. Hahn, E. L., Spin echoes. *Phys. Rev.*, 1950, **80**, 580.
9. Carr, H. Y. and Purcell, E. M., Effects of diffusion on free precession in nuclear magnetic resonance experiments. *Phys. Rev.*, 1954, **94**, 630.
10. Torrey, H. C., Bloch equations with diffusion terms. *Phys. Rev.*, 1956, **104**, 563.
11. Callaghan, P. T., *Principles of Nuclear Magnetic Resonance Microscopy*. Clarendon Press, Oxford, 1983 (Chapter 9).
12. Touzo, B., Trumeau, D., Massiot, D., Farnan, I. and Coutures, J.-P., High temperature  $^{27}\text{Al}$  NMR time resolved study. Application to the CaO– $\text{Al}_2\text{O}_3$  binary system. *J. Chim. Phys.*, 1995, **92**, 1871–1876.
13. For description of this technique applied to temperature measurements in the diamond anvil cell, see Heinz, D. and Jeanloz, R., Temperature measurements in the laser-heated diamond cell. In *High Pressure Research in Mineral Physics*, ed. M. H. Manghni and Y. Syono. Terra Scientific, Tokyo, 1987, pp. 113–1274.
14. Jephcoat, A. P. and Besedin, S. P., Temperature measurement and melting determination in the laser-heated diamond-anvil cell. *Phil. Trans. R. Soc. Lond. A*, 1996, **354**, 1333–1360.
15. Weber, J. K. R., Nordine, P. C. and Krishnan, S., Effects of melt chemistry on the spectral absorption coefficient of molten aluminum oxide. *J. Am. Ceram. Soc.*, 1995, **78**, 3067–3071.
16. Coutures, J.-P., Rifflet, J.-C., Florian, P. and Massiot, D., Etude par analyse thermique et par RMN très haute température de  $^{27}\text{Al}$  de la solidification de  $\text{Al}_2\text{O}_3$  en l'absence de nucléation hétérogène: effets de la température du liquide et de la pression partielle d'oxygène. *Rev. Int. Hautes Tempér. Réfract., Fr.*, 1994, **29**, 123–142.
17. Florian, P., Massiot, D., Poe, B., Farnan, I. and Coutures, J.-P., A time resolved  $^{27}\text{Al}$  NMR study of the cooling process of liquid alumina from 2450 °C to crystallization. *Solid State Nuclear Magn. Reson.*, 1995, **5**, 233–238.
18. Videa, M., Xu, W., Geil, B., Marzke, R. and Angell, C. A., High  $\text{Li}^+$  self-diffusivity and transport number in novel electrolyte solutions. *J. Electrochem. Soc.*, 2001, **148**, A1352–A1356.
19. Xu, W., Shusterman, A. J., Videa, M., Velikov, V., Marzke, R. and Angell, C. A., Structures of orthoborate anions and physical properties of their lithium salt nonaqueous solutions. *J. Electrochem. Soc.*, 2003, **150**, E74–E80.
20. Holz, M. and Weingartner, H., Calibration in accurate spin-echo self-diffusion measurements using  $^1\text{H}$  and less-common nuclei. *J. Magn. Reson.*, 1991, **92**, 115–125.
21. Rossin, R., Bersan, J. and Urbain, G., Viscosité de la silice fondue et de laitiers liquides appartenant au système  $\text{SiO}_2$ – $\text{Al}_2\text{O}_3$ . *C.R. Acad. Sci. Paris*, 1964, **258**, 562–564.
22. Scamehorn, C. A. and Angell, C. A., Viscosity-temperature relations and structure in fully polymerized aluminosilicate melts from ion dynamics simulations. *Geochim. Cosmochim. Acta*, 1991, **55**, 721–730.
23. Farnan, I., Oxygen bridges in molten glass. *Nature*, 1997, **390**, 14–15.

24. Stebbins, J. and Xu, Z., NMR evidence for excess non-bridging oxygen in an aluminosilicate glass. *Nature*, 1997, **390**, 60–62.
25. Poe, B. T., McMillan, P. F., Cotè, B., Massiot, D. and Coutures, J.-P., In-situ study by high-temperature  $^{27}\text{Al}$  NMR spectroscopy and molecular dynamics simulation. *J. Phys. Chem.*, 1992, **96**, 8220–8224.
26. Yarger, J. L., Smith, K. H., Nieman, R. A., Diefenbacher, J., Wolf, G. H., Poe, B. T. et al., Al coordination changes in high-pressure aluminosilicate liquids. *Science*, 1995, **270**, 1964–1967.
27. Weber, J. K. R., Anderson, C. D., Merkeley, D. R. and Nordine, P. C., Solidification behavior of undercooled liquid aluminum oxide. *J. Am. Ceram. Soc.*, 1995, **78**, 577–582.
28. Wang, T. C., Anilkumar, A. V., Lee, C. P. and Lin, K. C., Core-centering of compound drops in capillary oscillations: observations on USML-1 experiments in space. *J. Colloid Interface Sci.*, 1994, **165**, 19–31.
29. Kimmich, R., *NMR Tomography, Diffusometry and Relaxometry*. Springer-Verlag, Berlin, 1997 (Chapters 19, 23, 25, 29–31).
30. Klammler, F. and Kimmich, R., Volume-selective and spectroscopically resolved NMR investigation of diffusion and relaxation in fertilized hen eggs. *Phys. Med. Biol.*, 1990, **35**, 67–79.
31. Weis, J., Kimmich, R. and Müller, H.-P., NMR imaging of thermal convection patterns. *Magn. Reson. Imaging*, 1996, **14**, 319–327.
32. Nelson, L. S., Richardson, N. L., Keil, K. and Skaggs, S. R., Effects of argon and oxygen atmospheres on pendant drops of aluminum oxide melted with carbon dioxide laser radiation. *High Temp. Sci.*, 1973, **5**, 138–154.